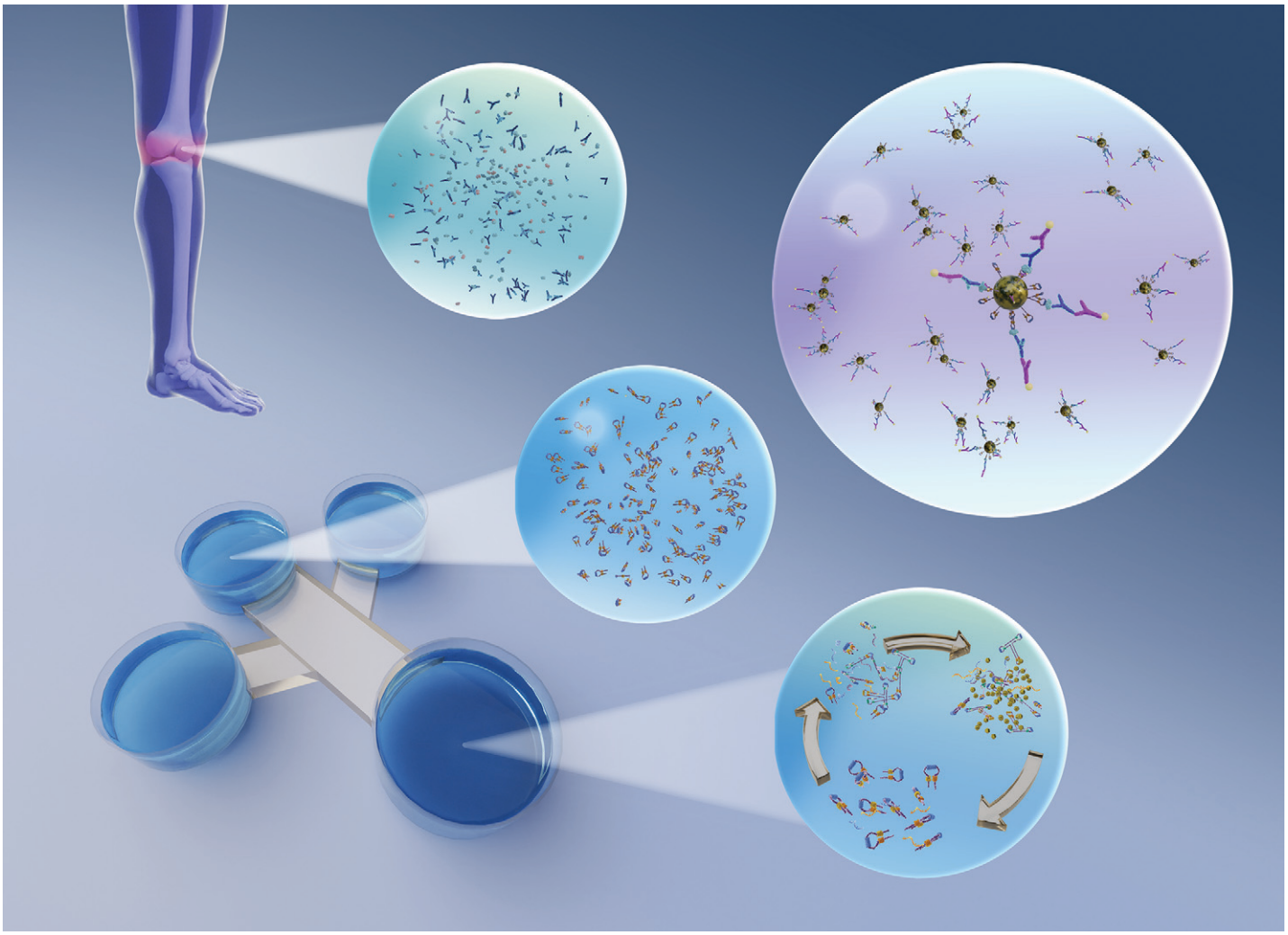

Featuring work from Microfluidic Biochips Lab of Professor Gwo-Bin "Vincent" Lee, National Tsing Hua University, Taiwan. We thank Mr. Terry Juang for improving the quality of the art work.

Aptamer selection against alpha-defensin human neutrophil peptide 1 on an integrated microfluidic system for diagnosis of periprosthetic joint infections

A novel integrated system for SELEX automation was developed to screen the aptamers specific to HNP 1 in diagnosing periprosthetic joint infection (PJI). A unique approach of positive+negative+competitive selection was performed for aptamer screening with high selectivity and specificity. The aptamer-based ELISA-like assay could significantly distinguish between synovial fluid of PJI (positive) and non-PJI patients (negative).

As featured in:

See Mel S. Lee, Gwo-Bin Lee *et al.*, *Lab Chip*, 2022, **22**, 250.

ROYAL SOCIETY OF CHEMISTRY

rsc.li/loc

Registered charity number: 207890

Lab on a Chip

PAPER

View Article Online
View Journal | View Issue

Cite this: *Lab Chip*, 2022, **22**, 250

Aptamer selection against alpha-defensin human neutrophil peptide 1 on an integrated microfluidic system for diagnosis of periprosthetic joint infections†‡

Rishabh Gandotra,[a] Hung-Bin Wu,[b] Priya Gopinathan,[b] Yi-Cheng Tsai,[b] Feng-Chih Kuo,[c] Mel S. Lee *[d] and Gwo-Bin Lee *[ab]

Periprosthetic joint infections (PJIs) arising from joint arthroplasty are dreadful, yet difficult to diagnose in subtle cases. Definite diagnosis requires microbiological culture to confirm the causative pathogens. However, up to 40% of culture-negative PJI needs other surrogate biomarkers such as human neutrophil peptide 1 (HNP 1) to improve diagnostic accuracy or gauge therapeutic responses. To devise a diagnostic method, systematic evolution of ligands by exponential enrichment (SELEX) (five rounds) was used to screen PJI biomarkers on a compact (20 × 20 × 35 cm), integrated microfluidic system equipped with two separate Peltier devices and one magnetic control module where an aptamer with high affinity and specificity for HNP 1, which has been used as one of the synovial fluid (SF) biomarkers for detecting PJI, was identified for the first time. Two rounds of negative selection (with immunoglobulin G & human serum album) on-chip followed by one round of unique "competitive selection" with SF extracted from PJI patients validated the specificity of the HNP 1 aptamer. The dissociation constant was measured to be 19 nM. The applicability of SF HNP 1 levels for diagnosing PJI was then verified by a new aptamer-based enzyme-linked immunosorbent assay (ELISA)-like assay. It is envisioned that this new aptamer and the associated assay could be used in future clinical applications.

Received 29th October 2021,
Accepted 7th December 2021

DOI: 10.1039/d1lc00969a

rsc.li/loc

Introduction

Total joint arthroplasty (TJA) is a surgical procedure in which a damaged or arthritic hip, knee, shoulder, wrist, or other joints are replaced with synthetic materials. Hip and knee TJA are the most common and account for 25% of TJA in those <65 years of age.[1,2] In the United States of America (USA) alone, one million TJA cases are performed annually and this is expected to increase to four million by 2030.[3] Despite being among the most successful procedures, complications are nevertheless reported; for instance, periprosthetic joint infections (PJIs) occur in 1–2% of all TJA instances. PJI induces several symptoms such as fever, acute pain, joint inflammation, functional incapacitation, and prolonged post-operative wound discharge; severe cases can even lead to death. According to previous studies, PJI has a five-year mortality rate of 22% and 21% for knee[4] and hip arthroplasties, respectively.[5] Prolonged, costly treatments can financially and emotionally burden PJI patients, due to the requirement of prompt intervention and costly procedures utilizing considerable resources; the treatment costs are expected to reach 1.85 billion USD annually by 2030 within the USA.[6]

Due to the non-specific nature of the symptoms, it is challenging to diagnose PJI though; pre-, intra-, and post-operative examinations of blood and synovial fluid (SF) must be undertaken.[7,8] Such tests are not practical in many cases since they are relatively costly, exhibit relatively low sensitivity/specificity and require time-consuming processes, meaning that an early diagnostic method tackling these issues is of great need. The Musculoskeletal Infection Society (MSIS) has deemed a standardized definition of PJI[9] and has further contributed to the 2013 International Consensus Meeting (ICM).[10] The

[a] *Institute of NanoEngineering and Microsystems, National Tsing Hua University, Hsinchu 30013, Taiwan*
[b] *Department of Power Mechanical Engineering, National Tsing Hua University, Hsinchu 30013, Taiwan. E-mail: gwobin@pme.nthu.edu.tw; Tel: +886 3 5715131 ext. 33765*
[c] *Department of Orthopaedic Surgery, Kaohsiung Chang Gung Memorial Hospital, Kaohsiung 83301, Taiwan*
[d] *Department of Orthopaedic Surgery, Paochien Hospital, Pingtung 90064, Taiwan. E-mail: bone@doctor.com; Tel: +886 8 766 5999 Ext. 7889*

† Preliminary results within this work were presented at the 25th International Conference on Miniaturized Systems for Chemistry and Life Sciences (μTAS 2021), October 10–14, 2021.

‡ Electronic supplementary information (ESI) available. See DOI: 10.1039/d1lc00969a

Rishabh Gandotra

Rishabh Gandotra received his B. Tech and M. Tech degrees from the Amity Institute of Nanotechnology at Amity University, Noida, India in 2017. Currently he is a PhD student in the Institute of NanoEngineering and Microsystems (iNEMS) at National Tsing Hua University, Taiwan. His research interests are nanobiotechnology, and microfluidics and its biomedical applications.

Hung-Bin Wu

Hung-Bin Wu received his BS degree from the Department of Mechanical Engineering at Tatung University in 2020. Currently he is a Master's student in the Department of Power Mechanical Engineering (PME) at National Tsing Hua University, Taiwan. His research interests are nanobiotechnology, microfluidics and mechatronics.

Priya Gopinathan

Priya Gopinathan received her BS degree from the Department of Biotechnology at Rajasthan University, India in 2006 and MS degree from the Department of Biotechnology at Bharathiar University, India in 2008. She received her PhD from the Institute of Nanoengineering and Microsystems at National Tsing Hua University, Taiwan in 2019. Currently, she is a post-doctoral fellow at the Department of Power Mechanical Engineering at National Tsing Hua University, Taiwan. Her research interests include in vitro diagnostics, bio-microfluidics, and molecular biology.

Yi-Cheng Tsai

Yi-Cheng Tsai received his BS and MS degrees from the Department of Life Science and the Institute of Biomedical sciences at Chang Gung University, Taiwan in 2007 and 2009, respectively. He completed his PhD study at the Graduate Institute of Biomedical Science, Division of Biochemistry, Molecular and Cellular Biology of Chang Gung University, Taiwan in 2014. Currently, he is a post-doctoral fellow in the Department of Power Mechanical Engineering at National Tsing Hua University, Taiwan. His research specialties are molecular biology, molecular diagnosis and nanobiotechnology.

Feng-Chih Kuo

Feng-Chih Kuo received his MD degree in 2005 from the Kaohsiung Medical University, Kaohsiung, Taiwan, and completed his orthopaedic training in 2011 at the Kaohsiung Chang Gung Memorial Hospital, Kaohsiung, Taiwan. He did his Post-Doctoral Research Fellowship Program with Prof. Parvizi at the Rothman Institute at Thomas Jefferson University Hospital from July 2017 to June 2018. He is currently an Associate Professor in the Department of Orthopaedic Surgery at Kaohsiung Chang Gung Memorial Hospital, Taiwan. His research interests focus on the diagnosis and treatment of periprosthetic joint infection and machine learning application in total joint arthroplasty.

Mel S. Lee

Mel S. Lee received his MD degree from Taipei Medical University in 1987 and Ph.D. degrees from the Graduate School of Clinical Medicine in Chang Gung University in 2001. He is a Professor in the Department of Orthopedic Surgery, Chang Gung Memorial Hospital and Superintendent of Paochien Hospital, Taiwan. His research interests focus on osteonecrosis, arthroplasty, periprosthetic joint infection, and joint preservation surgery.

provided data and definitions have been readily recognized worldwide among medical research groups and surgeons effectuating drastic improvements in diagnosis and course of treatment of PJI. A patient is identified with PJI if they meet the major criteria and minor criteria.[10] These definitions have been revised in the second ICM in 2018 and pre-operative diagnosis was further defined in order to identify PJI with satisfactory accuracy. One of such biomarkers with the highest score listed in the ICM list is SF under which positive alpha-defensins (AD) act as putative PJI biomarkers.[11] AD, including the human neutrophil protein (HNP), belong to a family of antimicrobial peptides that are released by neutrophils in response to pathogens.[12] Immunoassays for SF AD detection (HNP 1–3) are highly sensitive and specific, though normally only presence/absence data are yielded and show similarity with pre-operative results of the MSIS.[11] This makes it a powerful and potent biomarker in detecting PJI. Usually, the tests for AD are reported in terms of negative and positive tests. However, the sample-to-cutoff ratio and its absolute value are still under extensive investigation.[13] The major challenges in detection of human neutrophil peptide 1 (HNP 1) is the unavailability of simple test kits that most institutions lack despite their prospective utility. Furthermore, relying on mailing samples to specialized labs, which leads to relatively expensive and rigorous tests to obtain biomarker results, can hinder the prognosis of PJI patients.

Different domains of AD have been integrated into a certain ratio,[2] yet most antibodies target all three HNPs. Currently, the main focuses are on the combined properties of HNP 1–3, irrespective of the different behaviors of each among various diseases, due to readily available antibodies and similar domain structures promoting positive inflammatory responses.[15] The need to find a specific target protein as a biomarker in conditions like PJI is of utmost importance for faster detection and clear assessment. The most abundant species of the three peptides is HNP 1 as it comprises 50% of the total human AD.[14] There has been very limited work on the utility of HNP 1 alone as a biomarker[16,17] despite its potential in early detection of several diseases. However, according to the highest score of AD as a biomarker in PJI detection,[7] HNP 1 can play an important role in PJI detection. However, the reason why HNP 1 was restricted from being explored could be due to the lack of probes. Aptamers, single-stranded oligonucleotides that bind a variety of molecules with high affinity and specificity, could play this role, and their chemical stability and flexibility can be superior to those of antibodies if screened properly. Various advantages of aptamers have been reported over antibodies apart from similar structural alignment and functions.[18] For instance, the production of aptamers is cheap, fast and highly reproducible (*i.e.*, limited batch variations). They also offer lower immunogenicity and are highly selective and reversible with respect to 3D folding. All these advantages make aptamers a great candidate in order to replace antibodies with comparable or even superior performance.

Selection of aptamers is generally achieved by a process called "systematic evolution of ligands by exponential enrichment" (SELEX),[19,20] in which a random library of oligonucleotides is incubated with a target molecule. Then, protein–ligand interactions are exploited by repetitive rounds of binding, separation, and amplification such that a potential aptamer candidate is selected with high affinity and selectivity towards the target molecules.[21] Several methods involving magnetic beads for target immobilization for aptamer SELEX selection have been demonstrated.[22,23] Some of such approaches have been miniaturized to reduce labor and analysis times.[24] For instance, integrated microfluidic systems capable of carrying out on-chip SELEX have been developed,[31,32] and these (oftentimes) magnetic bead-based systems are characterized by reduced costs, shorter reaction times, minimal human intervention, and low sample/reagent volumes.[25,26] On-chip SELEX with positive aptamer selection was realized by our previously reported work which has demonstrated a system for semi-automatic selection of cardiovascular biomarkers.[27] The positive selection comes under the category of natural selection, where the beneficial alleles are promoted, *i.e.* in this study, oligonucleotides specific to the target protein (HNP 1). Other forms of selection are negative selection or purifying selection that hinders non-specific alleles (or proteins present in abundance in the sample) to enhance ssDNA selectivity. We hypothesized that we could improve upon this design by including negative and "competitive" selection steps to increase HNP 1 aptamer specificity in PJI SF on an improved version of a fully-automatic, integrated system such that a single microfluidic chip can be used for the complete SELEX process.

In this work, an aptamer specific to HNP 1 was selected for the very first time in order to identify PJI among the patients using an integrated microfluidic platform with an introduction to a newly established automated magnetic control module. The aptamers were successfully selected using the automated process of SELEX on a new integrated

Gwo-Bin Lee

Gwo-Bin Lee received his BS and MS degrees from the Department of Mechanical Engineering at National Taiwan University in 1989 and 1991, respectively. He received his PhD from the Department of Mechanical & Aerospace Engineering at the University of California, Los Angeles, USA in 1998. He is a Tsing Hua Chair Professor in the Department of Power Mechanical Engineering at National Tsing Hua University, Taiwan. His research interests focus on microfluidics, bio-sensing, nanobiotechnology and its biomedical applications.

microfluidic chip with two separate temperature regions *i.e.*, cooling region and heating region. These advancements made the new integrated device much better than our previously developed chip and system.[27] The developed microfluidic platform reduced the iteration rounds of SELEX from 15–20 rounds in the process[22,28] to only 5 rounds, consumed a lower volume of reagents and biological samples from an average of 100–300 μL (ref. 22 and 29) to only 50 μL and significantly minimized human intervention. For improving the specificity of the aptamers, a unique approach has been advanced by performing two negative selections (using immunoglobulin G (IgG) and human serum album (HSA)) after the five positive selections and then additional competitive selection by using the PJI positive clinical samples derived from the patients. The selected aptamer has demonstrated high binding affinity (with a dissociation constant of 19 nM) towards the target protein. Furthermore, this selected aptamer was tested in the assessment of clinical samples in SF which can promote the selected aptamer for clinical applications and enhance the research in replacing antibodies for future developments.

Materials and methods

On-chip SELEX

Fig. 1(a) depicts the schematic of on-chip SELEX for selection of HNP 1-specific aptamers using five positive, two negative and one competitive selection round. First, 100 μL of Dynabeads™ (M-450 Epoxy; 2×10^9 beads per mL, diameter = 4.5 μm; Invitrogen, USA) were suspended in 0.01 M sodium borate (binding buffer, pH 9; Merck, Germany) to 1 mL and coated with 20 μL of human HNP 1 (D2043; ≥80% purity by high-performance liquid chromatography (HPLC); 500 mg L^{-1}; Sigma-Aldrich, USA) and then blocked with ethanolamine (E9508; 0.5 % w/v; Sigma-Aldrich, USA) for 24 h at room temperature. Then, the beads were washed with 100 μL of 0.01 M phosphate buffered saline (PBS) (Merck, Germany) with 0.3% sodium azide (0.3 μL). The different micro-chambers of the chip (Fig. 2a; described below) were loaded with 1) 10 μL of 72-base pair (bp) single-stranded deoxyribonucleic acid (ssDNA) library (1 nM; made from a 1 μM stock from Medclub Scientific, Taiwan), 2) 10 μL of HNP 1-conjugated beads (~8.5×10^7 beads per mL), 3) 30 μL of 0.01 M PBS, 4) 200 μL of 0.01 M PBS + 0.01% Tween-20 (50 μL for each wash), and 5) 28 μL of polymerase chain reaction (PCR) reagents. The latter comprised PCR reagents (30 μL; 28 μL of original PCR reagents + 2 μL of ssDNA selected from the previous round) including 2 μL of target-specific oligonucleotide sequence products which were realized during thermo-release in the process of SELEX, 1.5 μL of forward primers (10 μM; 5′-ACAGCACCACAGACCA-40 random bp-TGTTTGTCTTCCTGCC-3′), 1.5 μL of reverse primers (10 μM; 5′-GGCAGGAAGACAAACA-40 random bp-TGGTCTGTGGT GCTGT-3′; both from Uni-Onward, Taiwan), 0.6 μL of deoxynucleotides (2.5 mM of each; Invitrogen), 0.2 μL of SuperTherm-Gold™ Taq polymerase (Bertec Enterprise, Taiwan), 3 μL of ST gold buffer (Bertec Enterprise), and 21.2 μL deionized water.

Next, SELEX for 5 rounds of positive selection was undertaken. First, the ssDNA library (10 μL) was denatured at 88 °C for 10 min in the ssDNA library chamber (heating region) of the chip. Then, the denatured ssDNA was transported to the transport chamber (cooling region), cooled to 10 °C for 1–2 min for single-strand regeneration, and transported back to the micromixer (Fig. 2a), where they were incubated with HNP 1-coated beads (10 μL) and binding buffer (30 μL) for 10 min. Note that two Peltier devices were used for heating and cooling, respectively (Fig. 2d). Next, the magnetic control module composed of a mechanical arm and an external magnet was employed to aggregate the magnetic beads at one corner of the micromixer, and the supernatant featuring unbound materials was discarded *via* the waste chamber. The beads were washed twice with washing buffer (50 μL), transported to the micromixer, and washed for 1 min

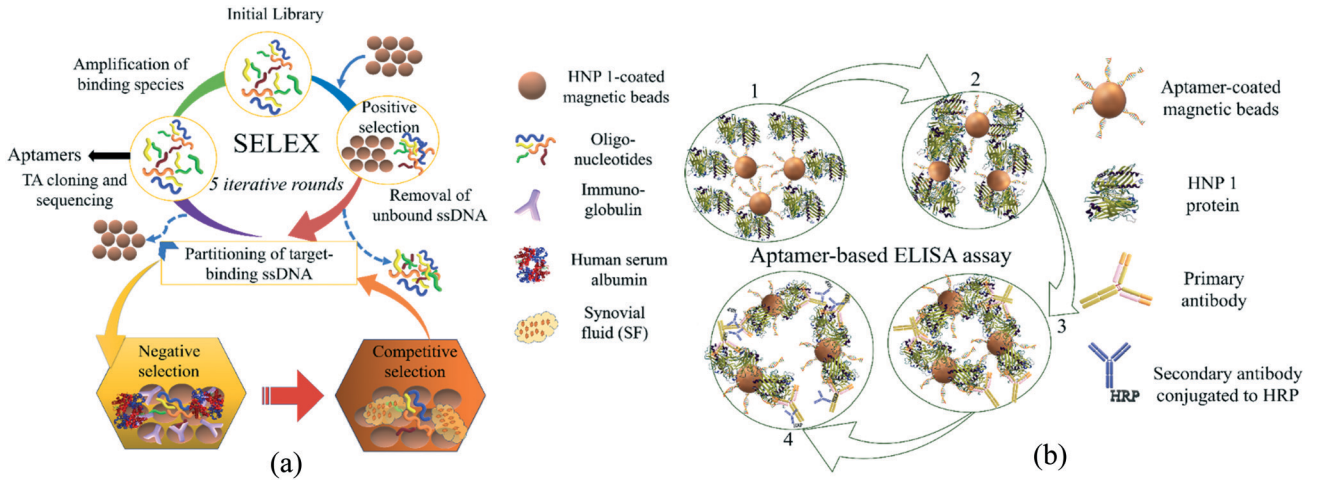

Fig. 1 (a) Schematic of SELEX featuring five positive, two negative (IgG & HSA), and one competitive (SF from PJI patients) selection round, respectively. (b) Schematic of an aptamer-based ELISA-like assay for measurement of HNP 1.

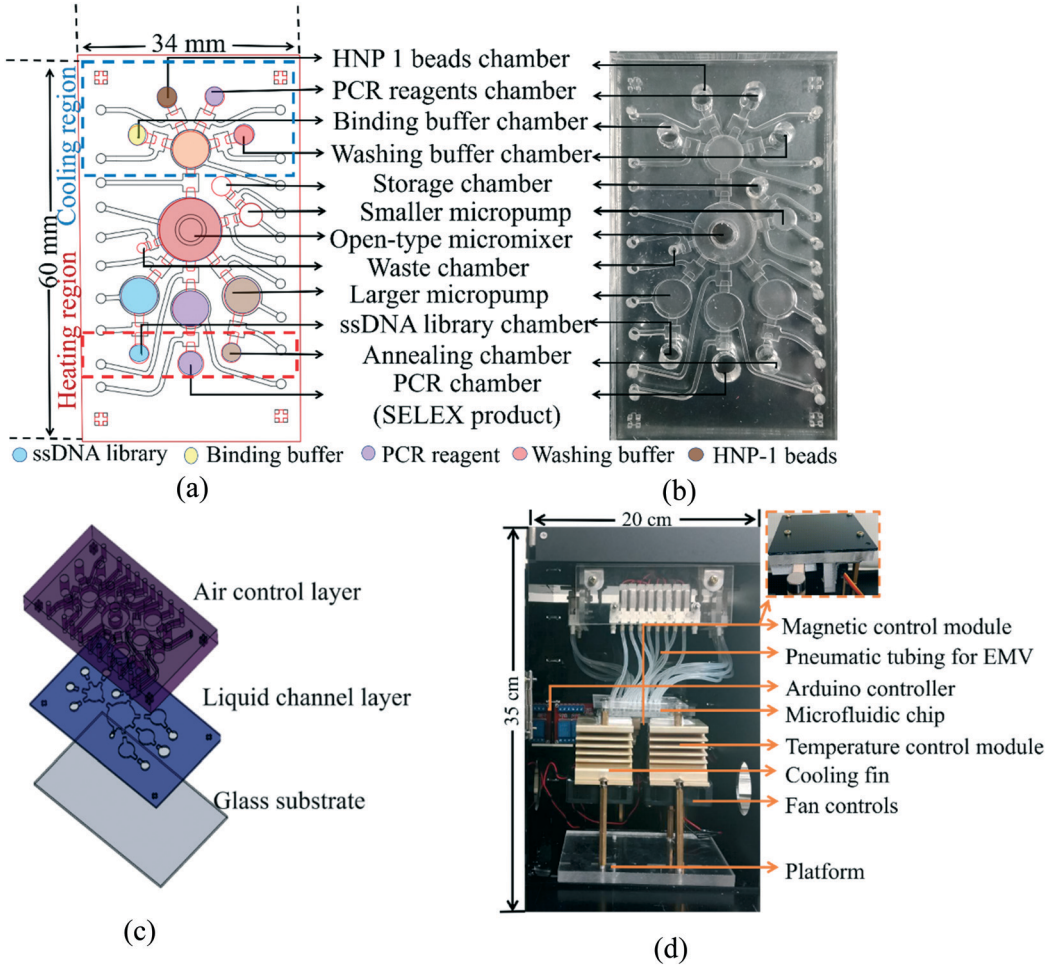

Fig. 2 (a) A schematic and (b) a photograph of the microfluidic chip for on-chip SELEX. (c) Exposed view of the three chip layers. (d) The automated microfluidic control system for automated SELEX. EMV = electromagnetic valve.

to remove unbound ssDNA. The beads were further resuspended in 20 μL of binding buffer, mixed for 1 min, and transported to the annealing chamber in the heating region for thermo-release (88 °C) of the target specific sequences from the beads. These products were then transported to the smaller transport unit and a storage chamber, where 2 μL were collected for PCR; the remainder was collected manually and analyzed off-chip by gel electrophoresis to confirm the selection process. Next, the 2 μL of ssDNA selected was mixed with PCR reagents (28 μL) from the PCR reagent chamber in the micromixer for 1 min before transporting to the PCR chamber. To ensure that no product evaporated during PCR, 20 μL of mineral oil was overlaid, and PCR was carried out as follows: 88 °C for 10 min followed by 20 cycles of 88 °C for 30 s, 60 °C for 15 s, and 72 °C for 30 s; a 7 min final elongation step was then carried out at 72 °C followed by a 10 °C ssDNA regeneration step (cooling region). Afterwards, 10 μL of PCR products were collected for further screening of the products, and 10 μL of sample were loaded into the ssDNA library chamber for the next round of SELEX after first washing the chip with washing buffer, 95% ethanol and double-distilled water (ddH_2O) and refilling the respective chambers with the reagents mentioned above and represented in Fig. 2b. It should be noted that collection and loading of samples before and after each round were performed manually; however, all the processes of SELEX on-chip including positive, negative and competitive selections with washing for each round were fully automated. Five rounds of positive selection were undertaken. Benchtop PCR was performed in the same manner for validation.

Negative selection, competitive selection, TA cloning and sequencing

Two rounds of negative selection with IgG and HSA were conducted after the aforementioned five positive selection rounds to deplete ssDNA that may exhibit high affinity towards these two abundant SF proteins (Fig. 1a), as advocated.[3] First, epoxy beads (100 μL) were coated with 8 μL of human IgG (I4506; 1 mg mL^{-1}, Sigma-Aldrich, USA) and 8 μL of human serum albumin (HSA; A3782; Fluka Analytical, Switzerland, 1 mg mL^{-1}), with 1 μL of bovine serum albumin (BSA, A7030l; 20 μM; Sigma-Aldrich) as the blocking reagent (see the ESI‡ for details). Then, the IgG-coated beads (3 μL), HSA-coated beads

(3 μL), and bare epoxy beads (3 μL; negative control) were loaded into their respective chambers, as were 21 μL of 0.1 M PBS and 20 μL of 5th round SELEX products (Fig. 2a).

SELEX products, PBS, and beads were mixed for 10 min in the micromixer with the beads collected as above. The supernatant was then collected and PCR amplified as the procedure defined above. This process was repeated twice, and from the final product, 20 μL was loaded into the ssDNA library chamber and the rest of the product was utilized for further screening. Note that the volumes of target specific sequences utilized for negative and competitive selections were kept higher than positive selections due to the presence of multiple double-stranded DNA that may not denature and regenerate to ssDNA after generating the final product of positive selections such that it can cause the aptamer candidate to amplify much lower than expected in the subsequent PCR process of selection.

The chip was washed before and after each round as mentioned above. After loading a fresh 21 μL of 0.1 M PBS in the binding buffer chamber, competitive selection was undertaken to enhance aptamer specificity *via* competition of HNP 1 beads (3 μL) as prepared above in the presence of SF-coated epoxy beads (3 μL). SF fluids used in coating were in their initial concentrations as extracted from patients and no dilutions were performed for bead coating, which was prepared using a similar process to that of other beads described above (see the ESI‡ for details). The aim of this competitive selection was to allow the competition between the magnetic bead and protein complex with the pre-screened HNP 1 specific oligonucleotides. This process allowed the selection of the high affinity aptamer sequences to be amplified further by PCR. The assay was performed in a low-volume condition (50 μL) such that the binding process could be much more efficient and saturation could be achieved; all beads were stored in the HNP 1 bead chamber (Fig. 2a) and mixed with the aforementioned PCR product. SELEX was then undertaken on-chip as described above, and the final PCR products were cloned (TOPO™ TA; Invitrogen) per the manufacturer's recommendations, with plasmids transfected into One Shot® Competent Cells (Life Technologies) and grown on lysogeny broth (LB)–ampicillin (0.1%) plates for 16 h. Select clones were sequenced by Genomics (Taiwan) as described in the ESI,‡ and their 2-D structure was assessed (Fig. S3‡). The purified aptamers used in the following experiments were then synthesized (Genomics) and labelled with 5′ biotin.

Design and microfabrication of the microfluidic chip

The microfluidic chip (6.0 cm [*L*] × 3.4 cm [*W*]; Fig. 2a and b) was connected to an integrated microfluidic control system (Fig. 2d) that featured a microfluidic control module, a temperature control module (with two Peltier devices), a magnetic control module, and an Arduino Uno controller (Fig. 2d). It was designed where the heating (for on-chip PCR & thermo-release & denaturing of ssDNA) and cooling regions (for ssDNA regeneration) were physically separated. The radius of the micromixer was 0.4 cm with a mixing microvalve concentric to the mixer designed with a width of 0.06 cm. The microfluidic chip consisted of one micromixer of radius 0.4 cm, four micropumps that acted as the "large transportation unit" with a radius of 0.3 cm and an extrusion depth of 0.15 cm, one micropump that served as the "small transportation unit" with a radius of 0.18 cm and an extrusion depth of 0.15 cm, 14 normally-closed microvalves, a waste chamber, four reagent chambers (HNP 1 bead chamber, washing buffer chamber, binding buffer chamber and PCR reagent chamber) in the cooling region of the chip, one ssDNA library chamber, one annealing chamber and one PCR chamber in the heating region (Fig. 2a and b). Note that ssDNA denaturation, annealing and PCR were carried out in the heating region, while buffers and reagents were stored in the cooling region to avoid degradation of the reagents. Furthermore, the separate Peltier device (127120-50; He-Ying Electronic Materials, Taiwan) for the ssDNA regeneration process may aid the manipulation of ssDNA introduced for the next round of selection which was a mild issue mentioned earlier.[27] It is worth noting that the new chip was equipped with 2 temperature control regions, namely a heating region and a cooling region (Fig. 2a) based on 2 different temperature modules (Peltier devices in the system). This helps us for better storage of reagents and minimal interference of the temperature control module. Apart from that, 3 separate heating chambers (ssDNA library chamber for denaturation, annealing chamber for thermo-release and PCR chamber) have been designed to be separated from each other to avoid chances of contamination *via* beads for each round. Overall, the newly developed chip resulted in efficient mixing, stable temperatures and low dead-volume of the reagents and products. This work has been differentiated from a previous work[27] significantly and made significant improvements as compared to the previous device.[27] One single chip can easily perform 5 rounds of positive selection, 2 rounds of negative selection and one round of competitive selection without human intervention.

On consideration of the pumping rate and the applied gauge pressure, it is worth noting that a pneumatically controlled microvalve with positive (compressed air) and negative (vacuum) gauge pressures established in our group previously was adopted.[27,31,32,39] The PDMS membrane for the air channel layer was deformed under the applied positive gauge pressure downwards and lifted (or deflected upwards) when a negative gauge pressure was applied; this mechanism leads to a precise amount of liquid to be transported in the respective chambers or mixers.

The microvalves were designed to prevent backflow of the unidirectional liquid, which would otherwise be an issue with reagents and viscous clinical samples like patient SF. Poiseuille's law for defining the dimensions of the transport chamber and the micromixer was followed to reduce hydraulic and flow resistance.[30] Short transport distances and curved, tapered edges helped in reducing "dead" volumes by

maintaining unidirectional flow. The microfluidic control module was composed of 20 electromagnetic valves (EMV, SMC 2070B-SBG-05; Wei-Chia Electro Materials, Taiwan) that enabled compressed air (TC-10; Centenary Material, Taiwan) or vacuum (DC-18V-12; Uni-Crown, Taiwan) to activate the large and small transport units (micropumps), which propelled reagents throughout the chip. A "servo" motor (MG995, Towerpro) with a gear-reciprocating mechanism was used to regulate the back-and-forth motion of the magnetic control module. The magnetic control module needed to align beads at one corner did not hinder any process due to the chip design and placement of the micromixer.

The three-layer microfluidic chip (Fig. 2c) was microfabricated from polymethyl methacrylate (PMMA) master molds under a computer-numerical-control (EGX-600, Roland Inc., Japan) machining process by using a drill bit of 0.5 mm.[31] The PMMA master molds were then used to generate the replicas for chip microfabrication. Chips were composed of three layers (Fig. 2c), including two polydimethylsiloxane (PDMS, Sylgard 184 A/B, Dow Corning, USA) layers and a glass substrate (G-Tech Optoelectronics Corp., Taiwan) (Fig. 2c).[27] The two PDMS layers were divided into the first layer known as the air control layer to control compressed air (or vacuum) through the air channel, while the second layer (liquid channel layer) was used to control the movement of liquid and its transportation in various chambers. Furthermore, the bottom glass substrate was used to seal the liquid channel. Both the PDMS layers were bonded together and then again bonded with the glass substrate using an oxygen plasma process at 90 W for 1 min (FC-12064, FEMTO, Science, USA).[32] More information on chip design and fabrication can be found in the ESI‡ (Fig. S1 and S2).

Determination of the dissociation constant (K_d)

Once the aptamer candidates were synthesized, their affinity and the equilibrium dissociation constant (K_d) of the selected aptamers against the target protein (HNP 1) were explored. A well-known and developed method using enzyme-linked immunosorbent assay (ELISA) was utilized in order to identify the K_d value of the aptamer,[33] which was originally used to explore the affinity of antigen–antibody equilibrium. The method was further modified and adapted for antibody affinity in the sub-nanomolar range and was considered a gold standard immunoassay for conventional ELISA.[34] It has been further modified to identify the K_d values of selected aptamers using ELISA-like assays.[35,36] The bead-based ELISA-like assay reported previously[31,32,37,38] was modified here in order to establish an assay for determining the K_d value. It should be noted that in order to study K_d, the concentration of the antigen–antibody (or aptamer–protein in our case) should be in the expected range of binding affinity and the dynamic range should be as low as possible as per the recommendations provided.[33,38] As shown in Fig. 1(b), 100 μL of magnetic beads (Dynabeads™ MyOne™ Streptavidin C1, ~8.5×10^9 beads per mL, Invitrogen, USA) were incubated with 5 μL of biotinylated aptamers (100 μM in PBS) for 30 min and blocked with 20 μM BSA (0.1 % w/v) in 95 μL of 0.01 M PBS buffer. The beads were washed twice and incubated overnight at 30 RPM on an RM-2 shaker (ELMI, Russia; C1 mode). The aptamer-coated magnetic beads were then washed, re-suspended in 100 μL of PBS, and incubated with HNP 1 at concentrations ranging from 3 to 300 nM (0.01–1 mg L^{-1}) as the affinity range for the aptamer to achieve saturation in 200 μL as the reaction volume. This means that buffers and diluted antibodies were maintained in the same volume throughout the assay. Then, they were incubated with 500-fold diluted primary HNP 1 antibody (GTX75048; Genetex, Taiwan) for 60 min. Afterwards, they were incubated with a 1 : 2500 dilution of goat anti-mouse IgG-horseradish peroxidase (HRP) secondary antibody (GTX213111-01; Genetex). The dilution factors of both antibodies were based on attempting to minimize 1) false-positive results and 2) early binding and saturation. The dilution factors were also adjusted such that HRP signals could be detected when resuspended in 1 : 1 PBS : luminol. Sample luminescence was detected under an ELISA reader (FLUOstar Omega; BMG LabTech, Germany) while running LumiGlow software. To determine the K_d, the luminescence intensities were plotted against the concentrations of HNP 1 using a non-linear regression analysis.[31] Detailed procedures for K_d measurement can be found in the ESI.‡

For the aptamer-based enzyme-linked immunosorbent assay (ELISA)-like assay (Fig. 1b), the reagents used were primary antibody (GTX75048, HNP 1 antibody, Genetex, Taiwan) with a dilution factor of 1 : 100–1 : 1000 based on the datasheet provided and reaction volume, and secondary antibody (GTX213111-01, goat anti-mouse IgG conjugated with HRP, Genetex, Taiwan) with a dilution factor of 1 : 1000–1 : 10 000 based on the datasheet for ELISA. The dilution factor was based on independent experiments, according to experimental conditions to avoid false-positive data and antibody saturation. Synthesis and preparation of 5′-biotin-labeled aptamers were adapted from Genomics (Taiwan) at a stock concentration of 100 μM (with an optical density of 5 absorbance units), suspended in 72 μL of 0.01 M PBS as mentioned in the datasheet and stored at −20 °C till further use.

An affinity measurement analysis was also carried out in order to confirm the aptamer specificity towards HNP 1 and non-target proteins (HSA & IgG) and its amplification was further investigated. The process followed the above-mentioned SELEX protocol with the same steps of denaturation, binding, thermo-release and PCR process for one single round where the synthesized aptamer sequence S9 was replaced by the ssDNA library. The beads used for the process were HNP 1-coated epoxy beads as mentioned above. The PCR of the thermo-released product from the beads after binding was performed for 3 different cycles (20, 15 & 10) to check the binding and amplification of the aptamer against the specific protein. A similar experiment was conducted with the epoxy beads coated with IgG and epoxy beads coated with HSA as prepared above for the process of negative selection. The process of SELEX was performed for different cycles (20,

15 and 10 cycles) to check the binding and amplification of the aptamer against the non-specific proteins.

An experiment was also introduced as another step for checking the binding efficiency of the aptamer candidate (S9) in comparison with scrambled aptamers (72 bp randomized sequence). The purpose of this experiment is to identify the selected aptamer affinity towards HNP 1. The details can be found in ESI‡ Fig. S5.

After determining the K_d, a similar protocol was used to develop a calibration curve for measurement of HNP 1. The assays were reproduced and replicated to assess the stability and sensitivity of the developed method. The detailed information for both the assays for evaluating the equilibrium dissociation constants and the calibration curve for measurement of HNP 1, reaction volume, dilution factor and other operating conditions could be found in detail in the ESI‡ (Table S1).

Aptamer-based ELISA-like assay of clinical samples

The aptamer-based ELISA-liked assay was used to analyze SF from four PJI-positive and four PJI-negative patients after TJA (from Chang Gung Memorial Hospital (CGMH), Kaohsiung, Taiwan; IRB no. 201802127B0). The identification of samples was verified using an established gold-standard protocol for HNP 1 detection for the assessment of clinical samples (Human alpha-Defensin 1 DuoSet ELISA, R&D Systems, Inc., USA). All experiments were performed in accordance with CGMH guidelines and approved by the CGMH ethics committee. Specificity tests in which patient SF was spiked with other proteins were performed to ensure that HNP 1 could still be quantified in the presence of other proteins present in SF (*e.g.*, IgG & HSA).

Briefly, at first, 100 μL of the streptavidin magnetic beads (with a concentration as described above, washed and resuspended in 92.5 μL of 0.01 M PBS buffer, pH 7.4) were incubated with biotinylated aptamers (7.5 μL of stock concentration (100 μM) with a similar process described to that above). A total reaction volume of 50 μL was used throughout the calibration process and all the buffers and antibodies were maintained at the same volume throughout the assay. For developing the calibration curve, samples were incubated with aptamer-coated magnetic beads at concentrations ranging from 0.1 mg L^{-1} to 100 mg L^{-1} (the dynamic range in PJI patients). Then, the above-mentioned primary antibody was used to bind the HNP 1 aptamers on magnetic beads at a 1 : 1000 dilution. Finally, 1 : 5000 dilution of the secondary antibody (as above) was incubated with the complexes, and the HRP signals were detected upon resuspension of 1 : 1 PBS : luminol on an ELISA plate reader as described above and the resultant values of HNP 1 were derived nearest to a threshold concentration of HNP 1 in PJI patients that helped assess the value of HNP 1 in clinical assays. The detailed protocol, which was essentially the same as that for K_d assessment, is described in the ESI‡ (notably Table S1).

Results and discussion

Efficacy of the micromixer, micropump and temperature control module

The micromixer was first characterized. The relationship between the mixing index[39] and mixing time (Fig. 3a) was assessed at different applied gauge pressures at a driving frequency of 1 or 2 Hz (n = 3), and the optimal conditions for efficient mixing were determined to be 2 Hz at positive and negative gauge pressures of 20 and −50 kPa, respectively (4 s). However, since the aptamer-based ELISA-like assay involves biological samples that could be sheared off, the driving frequency was reduced to 1 Hz for subsequent experiments (3.6 s). For the process from 1 Hz to 2 Hz, the key objective was to determine the mixing efficiency such that an efficient mixing could be achieved at the given parameters. However, due to the sensitive nature of the bead-based assay involving biological components, the shear force and stringency were kept to a minimum and the lowest range of the driving frequency to achieve a similar mixing efficiency was utilized as the optimum criterion of the micromixer. This ensured that ssDNA and protein molecules did not detach from the beads.[27]

The efficacy of the micropump was then explored. Herein, based on the membrane deflection mechanics,[40] it can be concluded that membrane deflection is directly proportional to the applied gauge pressure. This indicates that the capacity of the micropump to transport or inject liquid increases on increasing the applied gauge pressure. Fig. 4a and b show the relationship between the PBS pumping rate and driving frequency at variable gauge pressures for the large and small transport units. A

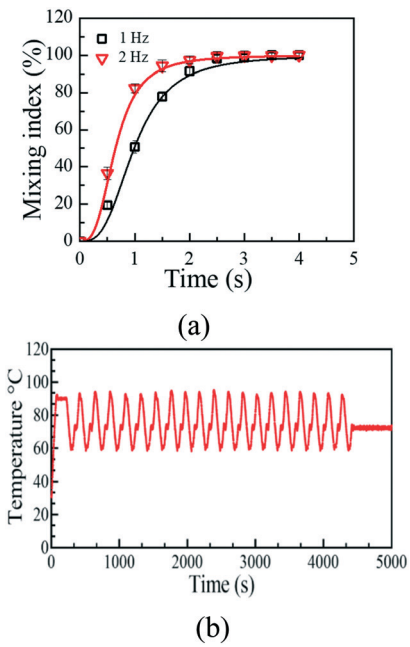

Fig. 3 (a) Mixing index of the micromixer (n = 3). (b) Temperature profile of on-chip PCR thermo-cycling.

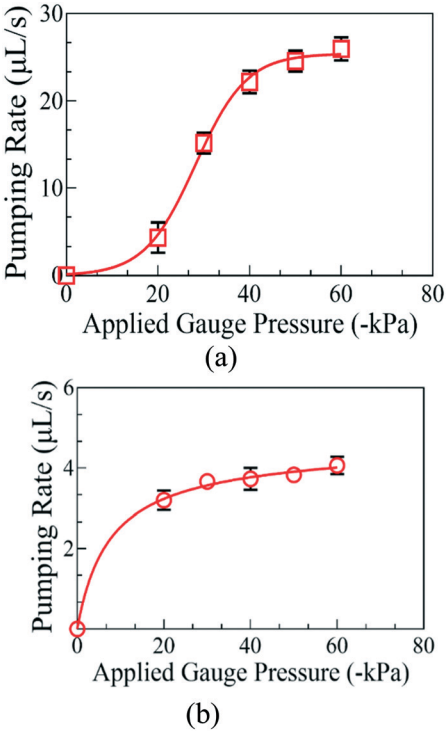

Fig. 4 (a) Pumping rate of micropumps #1 (large transport unit) and (b) #2 (small transport unit; n = 3 for each).

proportional increment was observed upon increasing the applied gauge pressure, with saturation reached at 26 μL s^{-1} (±0.5 [std. dev. for this & all other error terms]) at 60 kPa for the large transport unit and 4 μL s^{-1} (±0.1) at 60 kPa for the smaller one; this actually resulted in the membrane making contact with the substrate.

The temperature control module was next characterized (Fig. 3b) and the variation was found to be <2 °C. Thermal cycles for on-chip PCR could be successfully provided accordingly. We also advocate this novel stratified temperature design (*i.e.*, both heating and cooling regions) for those seeking to limit sample and reagent degradation on-chip.

On-chip SELEX and aptamer characterization

For the process of on-chip SELEX, 5 rounds of positive selection with the target protein HNP 1, 2 rounds of negative selection with two other abundant proteins in SF (IgG and HSA) and one round of competitive selection using SF from PJI patients were performed. After each round of SELEX, a 5 μL aliquot was collected from the storage chamber and analyzed by agarose gel electrophoresis (Fig. 5a). Note that 72-bp ssDNA was used as the positive control, while ddH_2O was used for the negative control. Initial SELEX rounds presented lower band intensities, though the intensities eventually rose to sufficient levels in only five rounds (Fig. 5a); this is far lower than the 15+ used in conventional SELEX,[22,24] indicating that on-chip SELEX is extremely efficient in selection of aptamers.

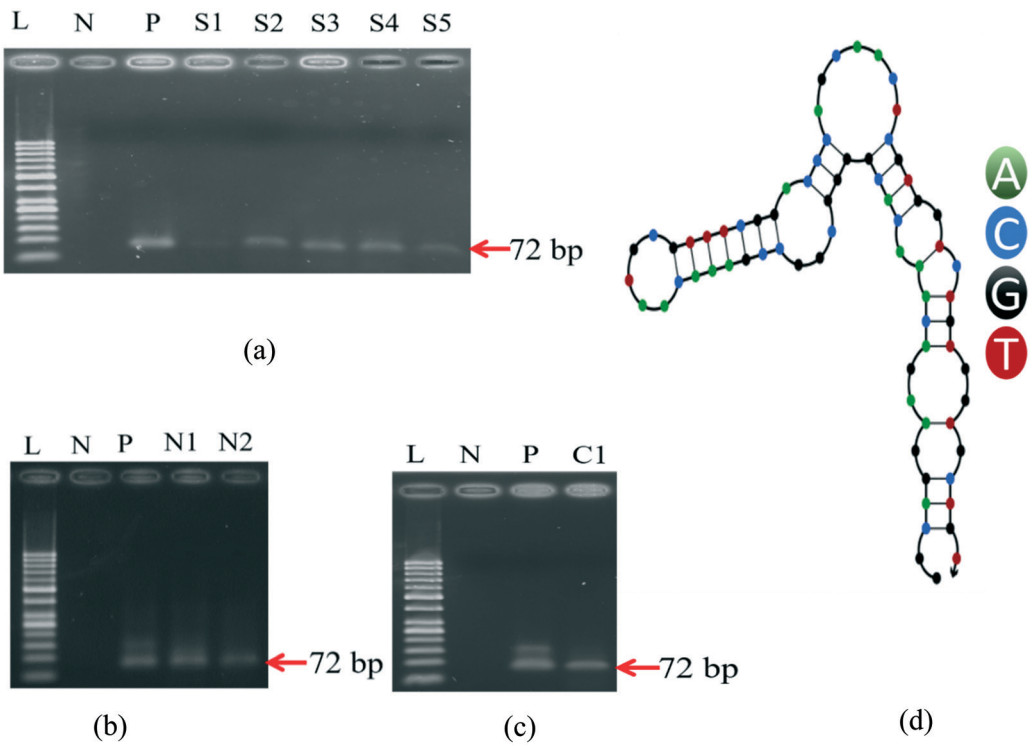

Fig. 5 (a) Agarose gel electrophoresis with EtBr staining of PCR products after five rounds (1–5) of positive selection *via* on-chip SELEX. (b) Two rounds of negative selection (N1 & N2). (c) One round of competitive selection for aptamer candidates (C1). In (a)–(c), L = 50-bp DNA ladder, N = negative control (ddH_2O), and P = positive control (1 nM ssDNA). (d) Predicted 2-D structure of the S9 aptamer.

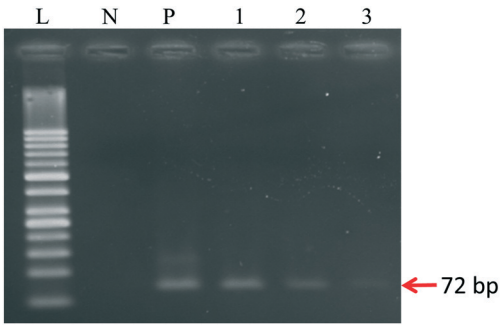

Fig. 6 Affinity tests for assessment of the S9 aptamer against HNP 1, L = 50-bp DNA ladder, N = negative control (ddH_2O), P = positive control, (1 nM ssDNA), 1 = 20 PCR cycles, 2 = 15 PCR and 3 = 10 PCR cycles.

When compared with our previous work on SELEX,[27] the current study increased the specificity of the selected aptamer by using two rounds of negative selection and one round of competitive selection using clinical samples (*i.e.* SF) for target proteins after five runs of positive selection. For negative selection, IgG and HSA were used since they are the two most abundant proteins in SF of PJI patients apart from AD[41] and SF as the biological compound for the competitive selection in the presence of purified HNP 1 where the abovementioned protocol was followed. Our positive + negative + competitive SELEX process not only eliminated the chance of binding of non-target proteins but also other biological compounds present in clinical samples, which could otherwise have caused issues with aptamer selectivity and sensitivity towards HNP 1. This newly developed approach helped us in making sure that the aptamer may have higher affinity and high specificity towards HNP 1 under clinical conditions similar to PJI. For this reason, a clear band was observed at 72 bp (Fig. 5b and c), even when using only 50 μL of reaction volume; this is far lower than that in prior work[29,42] and could result in cost savings.

The selected aptamer candidate (S9) was further analyzed by a nucleic acid package (NUPACK)[43] to assess its secondary structure and Gibb's free energy; it appears to represent a thermodynamically stable structure based on hydrogen bonding and various G–C pairings (Fig. 5d).

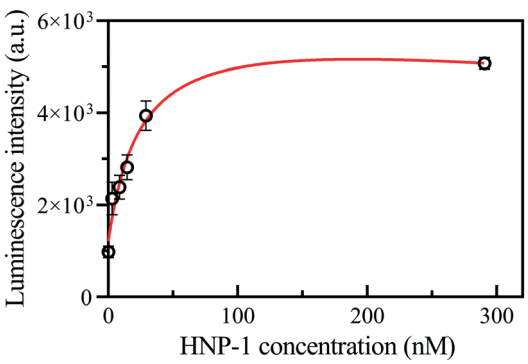

Fig. 7 Determination of the aptamer (S9) dissociation constant in an aptamer-based ELISA-like assay (n = 3).

An assay for assessment of aptamer affinity against HNP 1 was performed for different PCR cycles to confirm the binding with specific proteins (Fig. 6). A clear band was observed at 72-bp for HNP 1 that indicates successful amplification and binding of the aptamer towards the target protein at 3 different PCR cycles. Furthermore, no binding against non-specific proteins (IgG and HSA) was observed, indicating the high specificity of the screened aptamer (Fig. S4‡).

Upon regression analysis (Fig. 7), its K_d value was determined to be 19 nM (n = 3), which is comparable to commercially produced antibodies.[34,44] Note that proteins that possess greater isoelectric points have demonstrated higher chances of binding affinities in the range covering several tens to hundreds of nanomolar concentrations.[45,46] This is the first PJI-specific aptamer probe that has been developed; though other PJI biomarkers do exist,[7,11] the corresponding assays require larger reagent volumes, costly equipment, and are labor-intensive.

Analysis of clinical samples by the aptamer-based ELISA-like assay

In order to achieve the detection of the clinical samples, *i.e.* SF in our case extracted from PJI patients, an attempt to make sure of the specificity of the aptamer with regard to two of the major proteins present in SF including IgG and HSA was made while measuring HNP 1 to ensure the high affinity of the selected aptamer. An aptamer-based ELISA-like assay was employed for the assessment to cover the dynamic range for the estimated concentrations of HNP 1 among the PJI patients as a spike test. A similar assay has been demonstrated in our previous work for measurement of cardiovascular biomarkers[32,37] and has been recognized as a standard protocol for quantification of biomarkers for clinical samples. HPN-1, IgG, and HSA levels were therefore measured in patient SF using our new assay, and the relationship between protein concentration and optical intensity values (n = 3; Fig. 8a) depicts the affinity of the aptamer to HNP 1 and specificity to IgG and HSA. The graph was assessed using non-linear regression and a curve fitting equation that aided in estimating the HNP 1 detection threshold. A threshold value of 2.6 mg L^{-1} was obtained based 1) on our aptamer-based ELISA-like assay and 2) the fact that the threshold of HNP 1–3 of 5.2 mg L^{-2} was previously surmised to be two times greater than that of HNP 1 alone.[14] The calibration curve was established after validating the reproducibility and precision of the quantified target protein used in three repeats with a dynamic range 0.1–100 mg L^{-1}. With this approach, we calculated the HNP 1 levels in the four positive and negative PJI patients in a blind fashion (Fig. 8b). The concentrations demonstrate that the aptamer can easily distinguish between PJI and non-PJI patients and confirm the applicability of the selected aptamer in real biological samples. Using the diagnostic test evaluation calculator (Medcalc® – https://www.medcalc.org/calc/diagnostic_test.php), the sensitivity and specificity of the

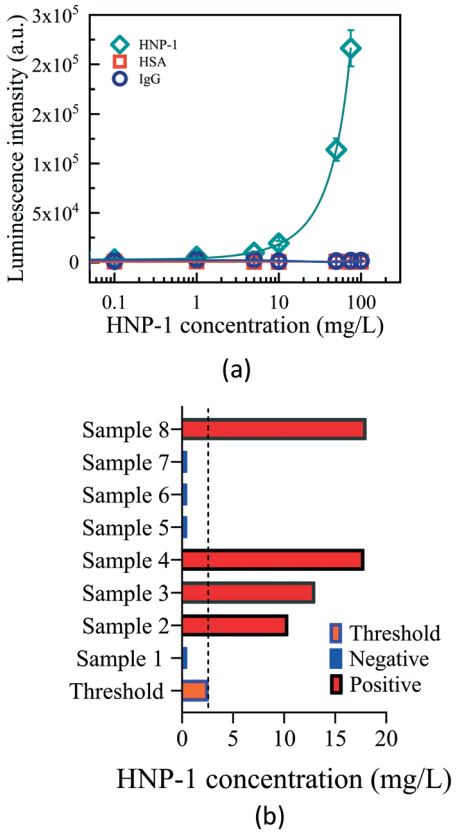

Fig. 8 (a) Specificity and selectivity tests for the aptamer-based ELISA-like assay for HNP 1, HSA, and IgG (n = 3). (b) HNP 1 measurements from the aptamer-based ELISA-like assay while using clinical PJI samples. The dotted line represents the threshold value, and samples 2, 3, 4, and 8 were patients experiencing PJI.

Table 1 Comparison between various established methods for PJI detection

Samples	Sensitivity & specificity	Time	Cost
Conventional ELISA[47]	100% & 95%	12–24 h	$$
Culture[47]	69% & 88%	48–96 h	$$
PCR[48]	86% & 91%	6–8 h	$$$
Aptamer-based ELISA-like assay	100% & 100%	<3 h	$

aptamer-based ELISA-like assay were determined to be 100% (95% CI 39.76% to 100.00%) with an accuracy of 100% (63.06% to 100.00%) for 8 tested samples. The presence of hemoglobulin or other blood interferents does not affect the reaction response of the ELISA results.[2] The quantitative assessment of the HNP 1 samples met the criteria defined by the MSIS.[10,11] The limit of detection (LOD) for HNP 1 was estimated to be 0.1 mg L^{-1} for the assay based on the calibration curve with several fold protein dilutions and 3 repeats of the assay. The LOD was verified in the clinical samples with negative results, as shown in Fig. 8b. A comparison table with several factors has been provided for PJI detection (Table 1) comparing several methods established for PJI detection. A table (ESI‡ Table S2) with detection ranges from commercialized products for alpha defensins[2,13,49] is provided in the ESI‡ with the available alpha defensin detection methods.

Conclusions

We demonstrated automated selection of an aptamer specific to HNP 1 *via* on-chip SELEX. It was achieved by using three modules for temperature control, flow control and magnetic control with highly efficient micro-devices. The automated magnetic control module was introduced for the first time on any reported microfluidic platform for precise control and alignment of magnetic beads with washing and thermo-release of oligonucleotides from the beads. All processes were automated for SELEX and the assay was characterized by reduced analysis time for the whole complete procedure (<12 h) and costs. The K_d of the selected aptamer was only 19 nM, comparable to an antibody, and it could distinguish between PJI-positive and negative SF samples. Consequently, this aptamer and the corresponding assay can be developed further for faster assessment, which could be used in point-of-care PJI diagnostics.

Author contributions

Rishabh Gandotra: conceptualization, data curation, formal analysis, investigation, methodology, validation, writing – original draft; Hung-Bin Wu: data curation, methodology, investigation; Priya Gopinathan: methodology, conceptualization; Yi-Cheng Tsai: methodology, conceptualization; Feng-Chih Kuo: resources, conceptualization, writing – proofreading, review and editing; Mel S. Lee: conceptualization, project administration, resources, writing – proofreading, review & editing; Gwo-Bin Lee: conceptualization, funding acquisition, methodology, project administration, resources, writing – proofreading, review & editing.

Conflicts of interest

There are no conflicts to declare.

Acknowledgements

The authors would like to thank the 1) Ministry of Science and Technology (MOST) of Taiwan (MOST 109-2221-E-007-006-MY3), 2) National Health Research Institutes of Taiwan (NHRI-EX110-11020EI), and 3) Chang Gung Memorial Hospital, Kaohsiung (Taiwan; CMRPG8K0501) for funding this work.

Notes and references

1 E. Gómez-Barrena and E. García-Rey, *J. Clin. Med.*, 2019, **8**, 1891–1893.
2 P. Melicherčík, E. Klapková, K. Kotaška, D. Jahoda, I. Landor and V. Čeřovský, *Diagnostics*, 2020, **10**(33), 1–10.
3 C. D. Etkin and B. D. Springer, *Arthroplast. Today*, 2017, **3**, 67–69.

4 Z. C. Lum, K. M. Natsuhara, T. J. Shelton, M. Giordani, G. C. Pereira and J. P. Meehan, *J. Arthroplasty*, 2018, **33**, 3783–3788.
5 K. M. Natsuhara, T. J. Shelton, J. P. Meehan and Z. C. Lum, *J. Arthroplasty*, 2019, **34**, S337–S342.
6 A. Premkumar, D. A. Kolin, K. X. Farley, J. M. Wilson, A. S. McLawhorn, M. B. Cross and P. K. Sculco, *J. Arthroplasty*, 2021, **36**, 1484–1489.
7 H. Abdelaziz, K. Rademacher, E. M. Suero, T. Gehrke, C. Lausmann, J. Salber and M. Citak, *J. Arthroplasty*, 2020, **35**, 2200–2203.
8 D. R. Osmon, E. F. Berbari, A. R. Berendt, D. Lew, W. Zimmerli, J. M. Steckelberg, N. Rao, A. Hanssen and W. R. Wilson, *Clin. Infect. Dis.*, 2013, **56**, e1–e25.
9 D. R. Osmon, E. F. Berbari, A. R. Berendt, D. Lew, W. Zimmerli, J. M. Steckelberg, N. Rao, A. Hanssen and W. R. Wilson, *Clin. Infect. Dis.*, 2013, **56**, 1–10.
10 J. Parvizi, T. Gehrke and A. F. Chen, *Zhongguo Gu Yu Guanjie Zazhi*, 2013, **95**, 1450–1452.
11 J. Parvizi, T. L. Tan, K. Goswami, C. Higuera, C. Della Valle, A. F. Chen and N. Shohat, *J. Arthroplasty*, 2018, **33**, 1309–1314.
12 T. Ganz, M. E. Selsted, D. Szklarek, S. S. Harwig, K. Daher, D. F. Bainton and R. I. Lehrer, *J. Clin. Invest.*, 1985, **76**, 1427–1435.
13 C. Deirmengian, K. Kardos, P. Kilmartin, S. Gulati, P. Citrano and R. E. Booth, *Clin. Orthop. Relat. Res.*, 2015, **473**, 2229–2235.
14 Y. Tsutsumi-Ishii, T. Hasebe and I. Nagaoka, *J. Immunol.*, 2000, **164**, 3264–3273.
15 J. Albrethsen, R. Bøgebo, S. Gammeltoft, J. Olsen, B. Winther and H. Raskov, *BMC Cancer*, 2005, **5**, 1–10.
16 R. Pero, M. Brancaccio, C. Mennitti, L. Gentile, A. Franco, S. Laneri, M. G. De Biasi, C. Pagliuca, R. Colicchio, P. Salvatore, G. D'Alicandro, D. Terracciano, M. Cennamo, E. La Civita, A. Liotti, C. Mazzaccara, G. Frisso, B. Lombardo and O. Scudiero, *Antibiotics*, 2020, **9**(306), 1–12.
17 C. Goebel, L. G. Mackay, E. R. Vickers and L. E. Mather, *Peptides*, 2000, **21**, 757–765.
18 S. Y. Toh, M. Citartan, S. C. B. Gopinath and T.-H. Tang, *Biosens. Bioelectron.*, 2015, **64**, 392–403.
19 C. Tuerk and L. Gold, *Science*, 1990, **249**, 505–510.
20 S. D. Jayasena, *Clin. Chem.*, 1999, **45**, 1628–1650.
21 S. C. B. Gopinath, *Anal. Bioanal. Chem.*, 2007, **387**, 171–182.
22 R. Ellingtontenburg, N. Nikolaus and B. Strehlitz, *J. Anal. Methods Chem.*, 2012, **2012**(415697), 1–14.
23 T. Hünniger, H. Wessels, C. Fischer, A. Paschke-Kratzin and M. Fischer, *Anal. Chem.*, 2014, **86**, 10940–10947.
24 M. Blind and M. Blank, *Mol. Ther.–Nucleic Acids*, 2015, **4**(e223), 1–7.
25 G. Hybarger, J. Bynum, R. F. Williams, J. J. Valdes and J. P. Chambers, *Anal. Bioanal. Chem.*, 2006, **384**, 191–198.
26 M. A. Gijs, F. Lacharme and U. Lehmann, *Chem. Rev.*, 2010, **110**, 1518–1563.
27 A. Sinha, P. Gopinathan, Y. D. Chung, H. Y. Lin, K. H. Li, H. P. Ma, P. C. Huang, S. C. Shiesh and G. B. Lee, *Biosens. Bioelectron.*, 2018, **122**, 104–112.
28 M. R. Dunn, R. M. Jimenez and J. C. Chaput, *Nat. Rev. Chem.*, 2017, **1**(10), 1–16.
29 M. Sypabekova, A. Bekmurzayeva, R. Wang, Y. Li, C. Nogues and D. Kanayeva, *Tuberculosis*, 2017, **104**, 70–78.
30 M. Jain and K. Nandakumar, *Biomicrofluidics*, 2010, **4**, 031101.
31 H.-I. Lin, C. C. Wu, C. H. Yang, K. W. Chang, G. B. Lee and S. C. Shiesh, *Lab Chip*, 2015, **15**, 486–494.
32 A. Sinha, P. Gopinathan, Y. D. Chung, S. C. Shiesh and G. B. Lee, *Lab Chip*, 2019, **19**, 1676–1685.
33 B. Friguet, A. F. Chaffotte, L. Djavadi-Ohaniance and M. E. Goldberg, *J. Immunol. Methods*, 1985, **77**(2), 305–319.
34 T. J. Vaughan, A. J. Williams, K. Pritchard, J. K. Osbourn, A. R. Pope, J. C. Earnshaw, J. McCafferty, R. A. Hodits, J. Wilton and K. S. Johnson, *Nat. Biotechnol.*, 1996, **14**, 309–314.
35 M. Vargas-Montes, N. Cardona, D. M. Moncada, D. A. Molina, Y. Zhang and J. E. Gómez-Marín, *Front. Cell. Infect. Microbiol.*, 2019, **9**(386), 1–13.
36 J. Faircloth, M. Moore, S. Stoufer, M. Kim and L.-A. Jaykus, *Viruses*, 2021, **13**(1716), 1–13.
37 P. Gopinathan, A. Sinha, Y. D. Chung, S. C. Shiesh and G. B. Lee, *Analyst*, 2019, **144**, 4943–4951.
38 K. H. Lee and H. Zeng, *Anal. Chem.*, 2017, **23**, 12743–12748.
39 C. Y. Lee, G. B. Lee, J. L. Lin, F. C. Huang and C. S. Liao, *J. Micromech. Microeng.*, 2005, **15**(1215), 1–10.
40 M. A. Eddings and B. K. Gale, *J. Micromech. Microeng.*, 2006, **16**, 2396–2402.
41 S. Ghosh, D. Choudhury, N. S. Das and B. Pingguan-Murphy, *Lubr. Sci.*, 2014, **26**, 387–410.
42 R. Stoltenburg, T. Schubert and B. Strehlitz, *PLoS One*, 2015, **10**, e0134403.
43 J. N. Zadeh, C. D. Steenberg, J. S. Bois, B. R. Wolfe, M. B. Pierce, A. R. Khan, R. M. Dirks and N. A. Pierce, *J. Comput. Chem.*, 2011, **32**, 170–173.
44 J. Bordeaux, A. W. Welsh, S. Agarwal, E. Killiam, M. T. Baquero, J. A. Hanna, V. K. Anagnostou and D. L. Rimm, *BioTechniques*, 2010, **48**, 197–209.
45 K. M. Ahmad, S. S. Oh, S. Kim, F. M. McClellen, Y. Xiao and H. T. Soh, *PLoS One*, 2011, **6**, e27051.
46 V. Codrea, M. Hayner, B. Hall, S. Jhaveri and A. Ellington, *Curr. Protoc. Nucleic Acid Chem.*, 2010, **40**, 9.5.1–9.5.23.
47 J. Bingham, H. Clarke, M. Spangehl, A. Schwartz, C. Beauchamp and B. Goldberg, *Clin. Orthop. Relat. Res.*, 2014, **472**, 4006–4009.
48 X. Qu, Z. Zhai, H. Li, H. Li, X. Liu, Z. Zhu, Y. Wang, G. Liu and K. Dai, *J. Clin. Microbiol.*, 2013, **51**, 2742–2746.
49 X. T. Tajima, T. Mori, F. Hirano, K. Sabanai, M. Kawasaki, Y. Yamanaka, M. Tsukamoto and A. Sakai, *J. UOEH*, 2020, **42**, 167–173.